IMA Journal of Applied Mathematics (2005) **70**, 666−676
doi:10.1093/imamat/hxh085
Advance Access publication on May 4, 2005

An experimental study of fixed points and chaos in the motion of spheres in a Stokes flow

T. MULLIN AND Y. LI
Manchester Centre for Nonlinear Dynamics,
University of Manchester, Oxford Road, Manchester M13 9PL, UK

C. DEL PINO
Department of Fluid Mechanics, University of Malaga, Spain

AND

J. ASHMORE
Department of Applied Mathematics & Theoretical Physics,
University of Cambridge, Wilberforce Road, Cambridge CB3 0WA, UK

We present the results of an investigation of a novel dynamical system in which one, two or three solid spheres are free to move in a horizontal rotating cylinder which is completely filled with a highly viscous fluid. At low rotation rates, steady motion is found where the balls adopt stable equilibrium positions rotating adjacent to the rising wall at a speed which is in agreement with available theory. At higher cylinder speeds time-dependent motion sets in via Hopf bifurcations, and when one or two balls are present the motion is strictly periodic. Perhaps surprisingly, it is found that three balls are required to produce low-dimensional chaos.

1. Introduction

The interaction between solid particles suspended in a viscous liquid in the Stokes flow limit is of considerable scientific and practical importance as discussed by Happel & Brenner (1965). Examples include particle interactions in colloids (Segre *et al.*, 1997), bioconvection (Pedley & Kessler, 1992), the motion of organisms (Orme *et al.*, 2003), the stability of arrays of particles with reference to ink jet printers (Crowley, 1971) and sedimentation processes (Peysson & Guazzelli, 2001). In the simplest of these flows, predictions from models suggest that three particles undergoing sedimentation will exhibit chaotic dynamics as discussed by Janosi *et al.* (1997). The chaos arises from particle–particle interaction and is transient in the unbounded flow of the model. It is interesting to ask whether this would be the case in a bounded domain and we believe our experiments shed some light on this possibility. A major mathematical difficulty then arises because a complete description of the motion of particles in Stokes flows is difficult when walls are nearby. Hence, walls are often ignored in theoretical studies of particle interactions, although their important effects have been considered more recently by Goren (1983), Brady (1988) and Dufresne *et al.* (2000). However, formulating a tractable mathematical model of the experiment under consideration here remains a formidable challenge.

We have constructed a Stokes flow experiment on a convenient laboratory scale and used it to investigate the interactions between individual particles and the walls as well as inter-particle coupling. The apparently simple physical system comprised a horizontal cylinder which was completely filled with glycerine, and experiments were performed using one, two and three steel balls which were free to move.

The balls are large and heavy and hence Brownian effects, which are important in many sedimentation processes, are negligible here. The cylinder is rotated at a constant speed such that the Reynolds number, Re, is typically of order one and hence the flow field is nearly Stokesian. Here $\mathrm{Re} = \frac{\omega r_c r_b}{\nu}$ where ω is the angular velocity of the cylinder of radius r_c, r_b is the radius of the ball and ν is the kinematic viscosity of the fluid. We have performed other sets of experiments using more viscous fluids such that the Reynolds number was reduced by a factor of approximately 40 and the results for both fixed-point and time-dependent motion (including chaos) were qualitatively unchanged, although the time-scales became proportionally longer. Here we focus on the results obtained with glycerine.

The positions of the balls were monitored as a function of the rotation rate of the cylinder which was set to prescribed values. Equilibrium points were observed for a wide range of rotation rates with each ball adopting a fixed location so that it rotated adjacent to the ascending wall. A lubrication layer existed between the ball and the wall and the gravitational force on the sphere was balanced by viscous forces in the thin liquid film. A photograph showing a front view of the apparatus, with three balls, is given in Fig. 1 and an overview of the different states is presented in Fig. 2. Above a critical rotation rate of the cylinder, the fixed-point behaviour gave way to periodic motion in the Y–Z plane for both a single and a pair of balls. The onset of time dependence occurred when the cylinder speed just exceeded the rate required to keep the balls at approximately mid-height of the cylinder and initially took the form of a small periodic oscillation above and below the mid-plane. At higher speeds, the amplitude of the oscillation grew and the ball was dragged up past mid-height before falling from the wall, landing further down and then dragged back up. Eventually, at high cylinder speeds, centrifugal effects dominated and solid body rotation was achieved so that the balls adhered to the wall at fixed locations.

A more interesting behaviour occurred with three balls where fixed points, periodic motion and low-dimensional chaos were observed over well-defined ranges of Re. In the time-dependent regime,

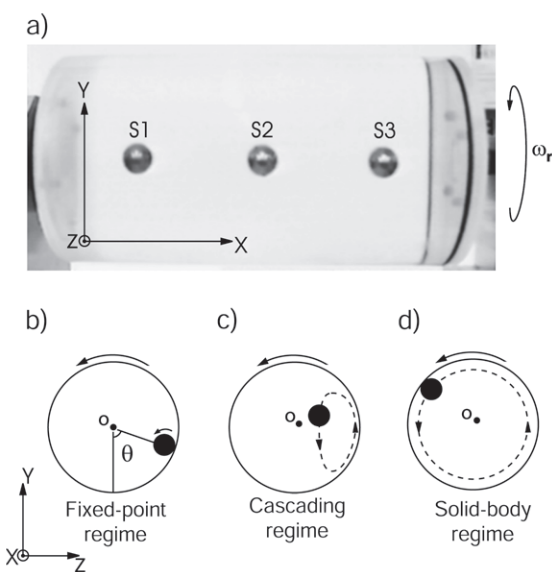

FIG. 1. (a) Front view of the apparatus showing the X, Y axes and labels used to identify the spheres S1, S2 and S3 which rotate at the shown fixed positions. The (b) the fixed-point, (c) cascading and (d) solid body regimes for a single ball are shown in the schematic below. A lubrication layer exists between the ball and the wall in (b). (Gap not shown.)

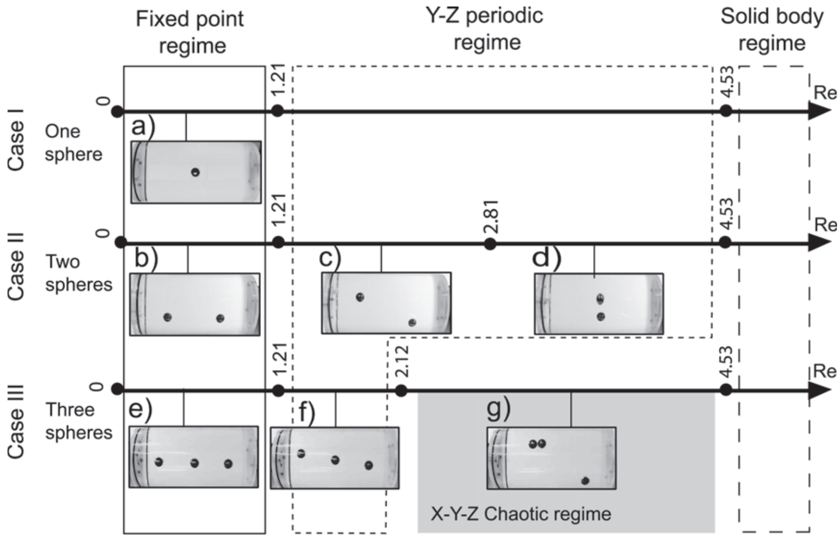

FIG. 2. Domain diagram with photographs superposed show typical behaviour for Case I (one ball), Case II (two balls) and Case III (three balls). The photographs illustrate examples of the dynamical states within the fixed-point (solid line), Y–Z periodic (dotted line), X–Y–Z chaotic (shaded) and solid body rotation regimes (dashed line). The critical Reynolds numbers which separate the regions are marked.

each ball acted as a local oscillator which was coupled to the others via the viscous medium during the falling phase of the sphere's motion. At a critical Re, this coupled oscillator system gave rise to a low-dimensional chaos which is in accord with dynamical systems theory (Baesens *et al.*, 1991; Terry *et al.*, 1999). One interesting feature of our experiment is that the presence of walls helps to sustain the chaos since particles cannot move far from each other. This is in contrast with the transient behaviour in the unbounded model of sedimentation for three particles by Janosi *et al.* (1997). Chaotic motion is found when the particles are close together but this ceases when one of the particles leaves the domain of influence of the others. In the system we consider, similar processes are likely to be involved when the spheres sediment but the chaos persists in our bounded domain. The effects are complicated by shear and rotation but serve as an illustration of chaotic motion in an apparently simple Stokes flow.

2. The experiment

The apparatus consisted of a 250-mm-long precision bored and polished Plexiglas cylinder of inner radius 59.00 ± 0.05 mm. The end caps of the cylinder contained centered ball races which were used to mount the cylinder with its axis accurately horizontal. The interior of the cylinder was filled with pure glycerine ($\rho = 1.26 \times 10^3$ kg m^{-3}) which had a measured kinematic viscosity of 936 ± 6 mm^2 s^{-1} at $22.3 \pm 0.1°$C, the controlled temperature. A small amount of Mearlmaid AA 'pearlessence' was added as a flow-visualizing agent in some experiments and viewing normal to an incident sheet of light enabled observation of the fluid motion. Results obtained with one, two and three 16-mm-diameter steel ($\rho = 7.8 \times 10^3$ kg m^{-3}) spheres are presented here, although glass and plastic balls were also used and the principal findings remain qualitatively the same (Mullin *et al.*, 2005).

The spheres were placed in the cylinder which was rotated at a constant angular velocity, ω, using a DC feedback controlled motor connected via a gear box and belt drive and the speed of the cylinder was monitored using an optical shaft encoder. The rotation rate of the balls was measured using a stop watch to time the passage of coloured marks on their surfaces via the cross-hairs of a travelling telescope. The marks were lightly applied and tests showed that they had a negligible effect on the motion. Measurements of the angle θ subtended by the balls were made using an engineers protractor aligned with the travelling telescope. The spatial locations of the spheres were recorded using a digital video technique and analysis of the dynamical motion was carried out off-line using a purpose-made image-processing software. This was used to identify the centres of the spheres and thereby extract positional time series.

3. Results

3.1 *Single sphere*

Consider first a single steel ball in the *fixed-point regime* which is Case I in the photograph in Fig. 2(a). At low Re, the sphere was located at an equilibrium point midway between the ends of the cylinder. The ball rotated smoothly adjacent to the ascending wall of the cylinder with a thin lubrication layer between the ball and the wall. As the rotation rate of the cylinder was increased the ball moved smoothly up the ascending wall to a new equilibrium point. As discussed below, the sine of the angle, θ, subtended by the ball varied approximately linearly with wall speed over a range of cylinder rotation rates. The linear relationship breaks down for angles less than approximately 10° when roughness effects become important. This is the subject of ongoing research and results will be published in due course by Mullin *et al.* (2005). Also, there is a clear departure from linearity for angles greater than 80°, just prior to the onset of time dependence. It is interesting to note that the surface speed of the cylinder required to maintain the ball in equilibrium was between a factor of two and eight less than its free-fall speed, i.e. the action of the wall was significant.

3.1.1 *A mathematical model* Establishing a tractable theoretical model for the complete flow field is difficult. However, we can make progress with the steady motion of a single sphere if we assume that the wall is locally planar and the finite size of outer flow does not have a significant effect. The closely related problem of the Stokes flow associated with a ball adjacent to a vertical wall in a semi-infinite expanse of fluid was first considered by Goldman *et al.* (1967). Their model requires modification when applied to particle motion adjacent to an inclined plane since the force normal to the boundary must be quantified. The symmetry of Stokes flows means that the pressure field generated in the lubrication layer is antisymmetric about the ambient pressure, and an important consequence is that there is no normal force exerted by the flow on the ball to balance its weight. Smart *et al.* (1993) included small inertial effects which break this symmetry and applied the model to a ball rolling down an inclined plane. They investigated both solid contact and fully lubricated flows for small particles (typical diameters were hundreds of microns) and obtained a good agreement between model and experiment. The effect of an applied linear shear on the lift force on the particles was later included by King & Leighton (1997).

More recently, Ashmore *et al.* (2005) have shown that for the larger particles typical of the present experiments, the pressure drops below the vapor pressure and generates a cavitation bubble in the diverging gap of the lubrication layer. This breaks the symmetry of the flow and provides sufficient normal force to balance the weight of the ball. The principle assumptions are that the flow is Stokesian, the outer flow is in solid body rotation and curvature effects of the cylinder wall are ignored. Justification of these assumptions and details of the model can be found in Ashmore *et al.* and we will only outline the essential aspects below.

The model comprises a sphere rotating at a rate ω in a semi-infinite bath of fluid adjacent to a planar boundary moving at velocity U inclined at an angle θ. The flow field is dominated by the motion in the narrow gap between the sphere and the wall since the minimum separation h_0 of the narrowest part of the gap is small compared to the sphere radius r_b. Hence, the characteristic length scale parallel to the boundary $(2h_0 r_b)^{1/2}$ is large compared to h_0 so that a lubrication approximation to Stokes equations is justified. A polar coordinate system (r, ϕ) is used on the boundary such that the origin is at the point of minimum separation between the sphere and the plane, and the angle ϕ is equal to zero on the line in the direction of the sphere's motion.

We denote the deviation from atmospheric pressure by $p(r, \phi)$, the difference between atmospheric and vapor pressure by p_b and the density difference by $\Delta\rho = \rho_s - \rho_f$. The model uses the force and torque balances on the sphere to calculate h_0, U and ω. Assuming that the tangential force and torque balances are not significantly affected by the small bubble, the results of Goldman *et al.* are valid:

$$\frac{8}{5}\mu\left(U - \frac{\omega r_b}{4}\right)\ln\left(\frac{r_b}{h_0}\right) + 3\mu(0.9588U + 0.2526\omega r_b) = \frac{2}{3}\Delta\rho g r_b^2 \sin\theta \tag{1}$$

$$\frac{1}{10}(U - 4\omega r_b)\ln\left(\frac{r_b}{h_0}\right) - 0.1895U - 0.3817\omega r_b = 0, \tag{2}$$

are the asymptotic expansions for the hydrodynamic force and torque where θ is the local angle of inclination of the boundary relative to the horizontal. First-order terms in the asymptotic expansion are retained as the expansion in $[\ln(r_b/h_0)]^{-1}$ converges relatively slowly.

The force balance normal to the plane is:

$$F_N = \int_0^{2\pi}\int_0^{r_b} pr\,\mathrm{d}r\,\mathrm{d}\phi = \frac{4\pi}{3}\Delta\rho g r_b^3 \cos\theta. \tag{3}$$

We approximate the pressure distribution using the lubrication pressure p_{lub} between a rotating sphere and a translating boundary, truncated at the vapor pressure to incorporate the effects of cavitation: $p(r, \phi) = \max\{p_{\mathrm{lub}}(r, \phi), -p_b\}$, where

$$p_{\mathrm{lub}}(r, \phi) = \frac{6\sqrt{2}\mu(U + \omega r_b) r_b^{1/2}}{5h_0^{3/2}} \frac{r}{(1 + r^2)^2} \cos\phi. \tag{4}$$

Equations (1)–(3) are solved using the Newton–Rhapson method to determine U, ω and h_0 for a specified value of the non-dimensional vapor pressure p_b. Further details are given in Ashmore *et al.*

3.2 *Comparison between theory and experiment for the steady motion of a single sphere*

We present a graph of the measured speed of the cylinder required to maintain the ball at a given angle θ plotted as a function of the angle in Fig. 3(a). The comparison between the experimental data points and the theory outlined above can be seen to be very good. A range of fixed points exist between $\sim 5°$ and $\sim 90°$ where the ball rotates adjacent to the wall with a thin lubrication layer which is predicted to be ≈ 10 μm thick. Unfortunately, we have no method of measuring the gap at present. The low angle limit is set by the roughness of the steel ball which is ≈ 2–3 μm and this interesting region is the subject of current investigation.

The rotation rate of the ball is slightly underestimated by the theory as can be seen in Fig. 3(b). The theoretical line has an average slope of ≈ 0.17, whereas the experimental estimate is ≈ 0.2. We believe that the small offset between the experimental and theoretical estimates of speed of rotation of the ball

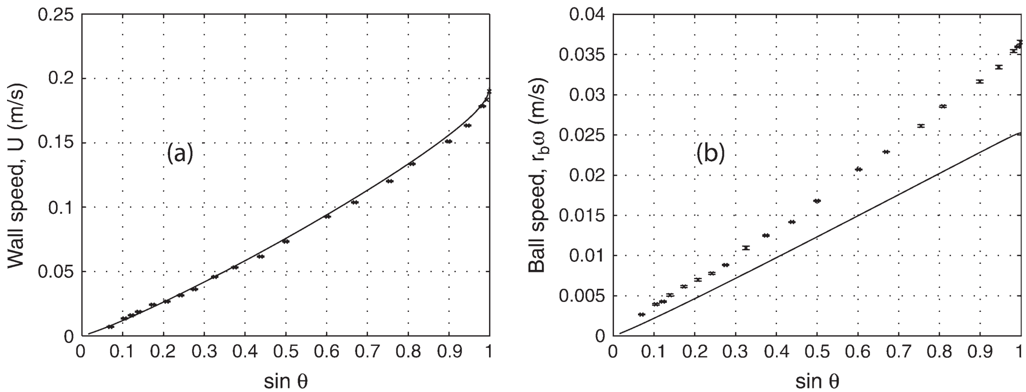

FIG. 3. Comparison between theory and experiment for cylinder and ball speeds plotted as a function of $\sin\theta$; (a) cylinder speed required to maintain the ball at a fixed point at given value of $\sin\theta$ (b) ball speed plotted as a function of $\sin\theta$.

may arise from neglecting the outer flow field as discussed by Goldman *et al.* (1967). Flow-visualization investigations showed that the bulk of the flow was in solid body rotation but the ball sat within a wake which propagated around the circumference of the cylinder. This complication could well be the source of the difference between theory and experiment. The conclusion we draw from the results presented in Fig. 3 is that a thin lubricating layer is formed between the sphere and the wall and cavitation plays a central role in providing the origins for a normal force.

3.3 *Onset of oscillations*

When the ball reached approximately mid-height ($\theta = 90^\circ$), the viscous force was insufficient to overcome the effects of gravity and small amplitude oscillations developed. In the case of a single ball, the periodic motion was strictly in the Y–Z plane midway between the two ends. Flow-visualization studies showed that the disturbances associated with this motion were local to the ball and located near the central plane. The ball moved up and down on a closed orbit as shown schematically in Fig. 1(c). The Y-projection of the oscillation of the ball was measured using the image-processing system and a plot of the square of this amplitude versus rotation rate is given in Fig. 4 for the case of the centre ball in the three spheres case. It can be seen that the constant level corresponding to the fixed point gives way to a square root growth in amplitude of the orbit for $\mathrm{Re} > 1.21$.

A sequence of segments of time series taken close to onset for the centre ball in the three spheres case is shown in Fig. 5. The first onset of oscillations had the same characteristic for one, two and three balls, i.e it was localized and showed the same growth behaviour. It may be seen that the onset of oscillations is initially intermittent so that long time series are required to obtain good averages of the amplitude. Bursting behaviour of this type is common in Hopf bifurcations in the presence of noise as discussed by Juel *et al.* (1997). We assume that the ‘noise’ in this case arises from surface roughness effects and it is interesting to note that there was no clear correlation between the bursting of individual spheres. Hence, the interaction was localized, unlike the free-fall motion discussed below, where strong correlation between the motion of individual spheres was evident. The amplitude of the oscillations increased in size as Re was increased such that the ball fell and was then dragged back up the ascending wall. The falling and rising phases of the motion are clear in the time series shown in Fig. 5 (d) where a distinct asymmetry has appeared.

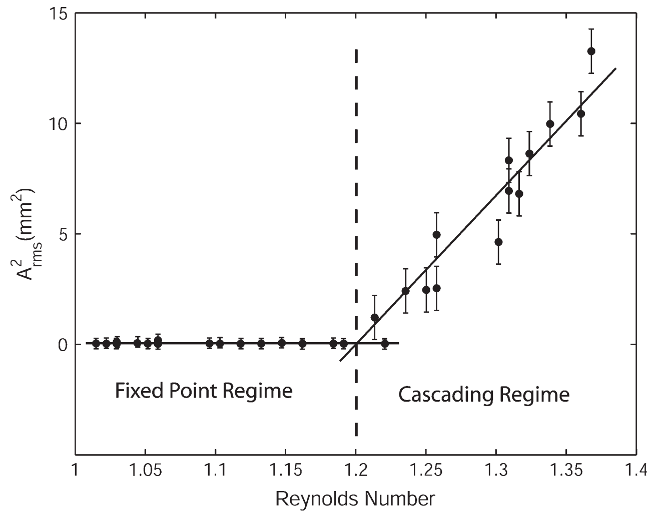

FIG. 4. The square of the amplitude of the Y oscillation plotted versus Reynolds number. Steady motion was found below Re = 1.21 and periodic above this value.

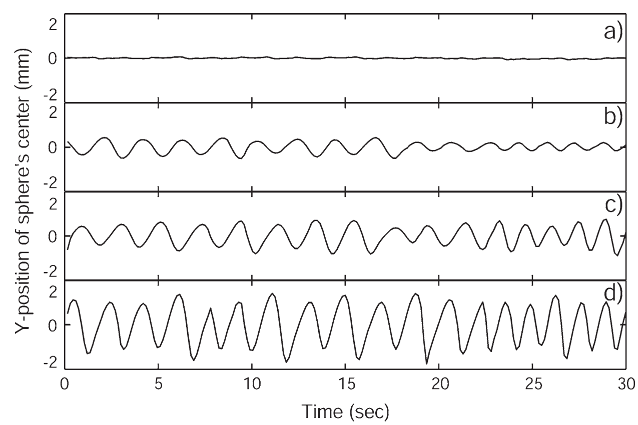

FIG. 5. The Y amplitude of the motion near the onset of oscillations. (a) Re = 1.19, (b) Re = 1.22, (c) Re = 1.24, (d) Re = 1.26.

In summary, the periodicity of the motion together with the square root dependence of the amplitude on the control parameter is consistent with a Hopf bifurcation (Strogatz, 1994). Clearly, the ball now has sufficient numbers of degrees of freedom for more complicated motions to occur and indeed chaos has been found for the case of a spheroid in a Stokes flow by Yarin *et al.* (1997). However, the motion was always singly periodic for the single sphere, although the cycle contained both 'free-fall' and 'wall-dominated' segments.

3.4 *Two balls*

We now compare the time-dependent motion, *cascading regime*, for $1.21 < \mathrm{Re} < 4.53$ for a single ball (Case I) and a pair of balls (Case II). The single ball oscillates at a fixed X location as shown

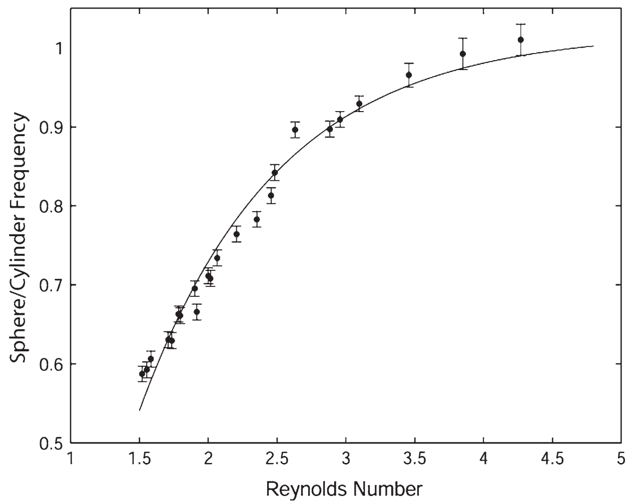

FIG. 6. Non-dimensional oscillation frequency of one and two balls versus Reynolds number. The least squares fitted line is an exponential.

in Fig. 2(a) and the amplitude of the oscillation grows until it equals the circumference of the cylinder. The frequency of the orbit grows until it matches that of the cylinder as shown in Fig. 6 where we combine the results for one and two balls. It can be seen that the ball and wall speeds eventually become equal at high rotation rates, i.e. the sphere does not move relative to the wall.

One of the fixed-point configurations for two balls is shown in the photograph of Fig. 2(b) where the balls are approximately six diameters apart and two diameters from the ends. Each of the balls acted in isolation and had the same speed ratio between ball and cylinder as in the single ball case shown in Fig. 3 (b). Another set of fixed points was possible with two touching spheres located midway along the cylinder (Li *et al.*, 2005). This non-uniqueness in the steady states disappeared at the onset of oscillations so that the photograph shown in Fig. 2(c) is representative of the dynamical behaviour over a range of Re.

An interesting aspect of the dynamical motion of two balls was that, while it was always strictly periodic, the two equally spaced balls oscillated such that they were locked in anti-phase as in the photograph of Fig. 2(c) and this persisted over the range of Re from 1.21 to 2.81. The stability of this motion was tested by briefly stopping one of the balls using a magnet and noting that the anti-phase motion returned immediately when the magnet was removed. Hence, this system provides an example of a spatially extended coupled oscillator in a viscous flow where the coupling is provided by the dynamic long-range interactions between moving particles (Feng & Joseph, 1995).

When Re was increased to 2.81 the anti-phase state became unstable and both balls moved to the mid-length position and rotated around each other in the mid-plane as shown in Fig. 2(d). This transition was reversible so that reduction in rotation rate led to the separated anti-phase state being regained after a transient. Yet, a further increase in Re led to the balls becoming attached to opposite sides of the wall and moving in solid body rotation as in the case of the single ball. Hence, as with the single ball, there was a sequence of steady states, periodic motion and solid body rotation as Re was increased.

3.5 *Three balls*

We now turn to a discussion of the experiment with three balls, which is Case III in Fig. 2. For Re $<$ 1.21, each ball acted as if in isolation and, as in the single sphere case, the ratio of the rotation speeds was 0.19. As with two balls, there was multiplicity in the fixed-point configurations (Li *et al.*, 2005) which disappeared at the onset of oscillations so that, within the range $1.21 < \mathrm{Re} < 2.12$, the state shown in the photograph of Fig. 2(f) was observed.

The onset of simply periodic motion occurred at a Hopf bifurcation at $\mathrm{Re} = 1.21$ as in the case of single and pair of balls. The motion of the outer two balls was in anti-phase, while the phase of the central one was intermediate as indicated in the snapshot shown in Fig. 2(f). Flow visualization showed that the disturbance generated by the balls was localized around each of them. The periodic motion persisted with increasing Re up to $\mathrm{Re} = 2.12$. At this critical value of Re, a reversible transition took place such that the balls began to wander erratically in the X direction, i.e. *along* the cylinder. This was superposed on the established motion in the Y–Z plane so that, unlike the cases of one and two balls, fully 3D motion was observed. A snapshot of this motion is shown in Fig. 2(g) where two balls have collided on the left-hand side of the cylinder.

The motion was no longer periodic and took the form of a chaotic longitudinal drift of the balls. A characteristic speed of this drift in the X direction was approximately 1 mm s^{-1} and was hence two orders of magnitude smaller than the circumferential motion. It was quite unlike that observed with two balls where all the sustained dynamics took place in the Y–Z plane alone. Now more degrees of freedom of the system were explored by the balls and spatio-temporal chaos was observed.

We show in Fig. 7 a 400-s segment of the X component time series for all three balls. The irregularity of the motion in this short segment is clear and contrasts sharply with the single and two ball cases where only periodic motion in the Y–Z plane was observed with no persistent motion in the X direction. The smallest lateral gaps in the time sequences correspond to the diameter of the spheres and are hence the closest points of approach of any two spheres. It is also interesting to note that there is motion of the third isolated sphere in the X direction when the other pair meet. Much longer time sequences recorded for periods of several hours confirmed this irregularity. Increase in Re over the range $2.12 < \mathrm{Re} < 4.53$, labelled *chaotic regime* in Fig. 2, leads to increasingly complicated motion before solid body motion sets in at $\mathrm{Re} = 4.53$. Here, the rotation rate was fast enough to overcome the effects of gravity so that the three balls remained at fixed locations on the cylinder wall.

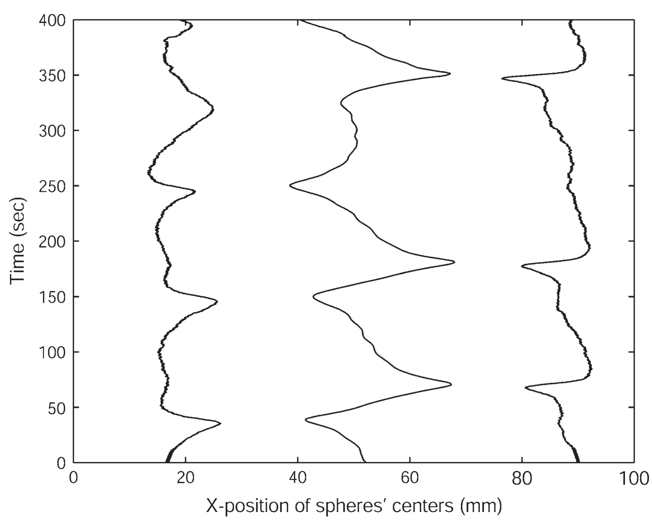

FIG. 7. A 400-s segment of the X component time series for the three spheres. The lateral motion is irregular when viewed on longer time-scales. The interaction between all spheres is evident.

4. Summary

A rich variety of interesting behaviour has been uncovered in this simple physical flow which is close to the Stokes limit. The steady behaviour for all configurations (one, two and three balls) is in surprisingly good quantitative agreement with available theory. Time dependence arises via a Hopf bifurcation and is strictly periodic for one or two balls. Perhaps, the most interesting aspect of all is that the interaction of three spheres in a Stokes flow moving under constant external forcing has provided a striking example of an apparently simple physical system which displays sustained low-dimensional spatio-temporal chaos in a non-trivial way. The non-linearity arises through the particle–particle and particle–wall interactions and the chaos is robust. These results are in accord with the transient behaviour found in simulations of three particle interactions in an unbounded sedimenting flow by Janosi *et al.* (1997), suggesting that the inclusion of walls may lead to a persistent behaviour. Thus, the observed phenomena may be of relevance to a wide variety of particulate flows. The device may also have relevance in chaotic mixers of very viscous fluids as discussed by Finn & Cox (2001).

Acknowledgements

The authors are grateful to M. Brenner, J. Hinch, D. Joseph, J. Rallison and, in particular, H. Stone for insightful discussions on these results. They are also grateful to P. M. Reis who processed the chaotic data and J. Seddon who carefully read the manuscript. The research of TM is supported by an EPSRC Senior Fellowship and he is grateful to the Isaac Newton Institute where this work was completed. The work of CP is supported by a grant from the Andalusian Government, LY by a grant from the Chinese Government and JA by a grant from the Leverhulme Trust.

References

ASHMORE, J., DEL PINO, C. & MULLIN, T. (2005) Cavitation in a lubrication flow between a moving sphere and a boundary. *Phys. Rev. Lett.*, **94**, 124501.

BAESENS, C., GUCKENHEIMER, J., KIM, S. & MACKAY, R. S. (1991) Three coupled oscillators mode-locking, global bifurcations and toroidal chaos. *Physica D*, **49**, 387–475.

BRADY, J. F. (1988) Stokesian dynamics. *Annu. Rev. Fluid Mech.*, **20**, 111–157.

CROWLEY, J. M. (1971) Viscosity-induced instability of a one–dimensional lattice of falling spheres. *J. Fluid Mech.*, **45**, 151–159.

DUFRESNE, E. R., SQUIRES, T. M., BRENNER, M. P. & GRIER, D. G. (2000) Hydrodynamic coupling of two Brownian spheres to a planar surface. *Phys. Rev. Lett.*, **85**, 3317–3320.

FENG, J. & JOSEPH, D. D. (1995) The unsteady motion of solid bodies in creeping flows. *J. Fluid Mech.*, **303**, 83–102.

FINN, M. D. & COX, S. M. (2001) Stokes flow in a mixer with changing geometry. *J. Eng. Math.*, **41**, 75–99.

GOLDMAN, A. J., COX, R. J. & BRENNER, H. (1967) Slow viscous motion of a sphere parallel to a plane wall–I. Motion through a quiescent fluid. *Chem. Eng. Sci.*, **22**, 637–653.

GOREN, S. L. (1983) Resistance and stability of a line of particles moving near a wall. *J. Fluid Mech.*, **132**, 185–196.

HAPPEL, J. & BRENNER, H. (1965) *Low Reynolds Number Hydrodynamics*. Englewood Cliffs, NJ: Prentice Hall.

JANOSI, I. M., TEL, T., WOLF, D. E. & GALLAS, J. A. C. (1997) Chaotic particle dynamics in viscous flows: the three particle Stokeslet problem. *Phys. Rev. E*, **56**, 2858–2868.

JUEL, A., DARBYSHIRE, A. & MULLIN, T. (1997) Dynamics induced by the effects of noise near bifurcation points. *Proc. R. Soc. Lond.*, **A453**, 2627–2647.

KING, M. R. & LEIGHTON, D. T. (1997) Measurement of the inertial lift on a moving sphere in contact with a plane in a shear flow. *Phys. Fluids*, **9**, 1248–1255.

LI Y., MULLIN, T., SEDDON J., DEL PINO C. & ASHMORE, J. (2005) The motion of a rough particle in a Stokes flow near to a boundary. (To be submitted to *J. Fluid Mech.*)

ORME, B. A. A., BLAKE, J. R. & OTTO, S. R. (2003) Modelling the motion of particles around choanoflagellates. *J. Fluid Mech.*, **475**, 333–355.

PEDLEY, T. J. & KESSLER, J. O. (1992) Hydrodynamic phenomena in suspensions of swimming organisms. *Annu. Rev. Fluid Mech.*, **24**, 313–358.

PEYSSON, Y. & GUAZZELLI, E. (2001) Velocity fluctuations in a bidisperse sedimenting suspension. *Phys. Fluids*, **11**, 1953–1955.

SEGRE, P. N., HERBOLZHEIMER, E. & CHAIKIN, P. M. (1997) Long-range correlations in sedimentation. *Phys. Rev. Lett.*, **79**, 2574–2577.

SMART, J. R., BEIMFOHR, S. & LEIGHTON, D. T. (1993) Measurement of the translational and rotational velocities of a noncolloidal sphere rolling down an inclined plane at low Reynolds numbers. *Phys. Fluids*, **5**, 13–24.

STROGATZ, S. H. (1994) *Nonlinear Dynamics and Chaos*. Perseus Books, p. 264. Reading, MA: Addison-Wesley.

TERRY, J. R., THORBURG, K. S., DESHAZAR, D. J., VANWINGEREN, G. D., ZHU, S., ASHWIN, P. & ROY, R. (1999) Synchronisation of chaos in an array of three lasers. *Phys. Rev. E*, **59**, 4036–4043.

YARIN, A. L., GOTTLIEB, O. & ROISMAN, I. V. (1997) Chaotic rotation of triaxial ellipsoids in simple shear flow. *J. Fluid Mech.*, **340**, 83–100.